

Particle-in-cell plasma simulation with OmpSs-2

Rodrigo Arias Mallo

June 7, 2019

Contents

1	Introduction	5
1.1	Motivation	5
1.2	Objectives	5
1.3	Context	5
1.4	Structure	5
2	Related work	7
I	Theory	9
3	Plasma introduction	11
4	Plasma simulation	13
4.1	The particle-in-cell method	13
4.2	Particle mover	13
4.2.1	Boris integrator	13
4.3	Charge accumulation	14
4.4	Field equations	14
5	Discrete model	15
5.1	Charge assignment	15
5.2	Field equations	16
5.2.1	Electric potential	16
5.2.2	LU decomposition	16
5.2.3	Multiple Fourier Transform (MFT)	17
5.2.4	Electric field	18
5.3	Force interpolation	18
5.4	Equations of motion	19
5.4.1	Boris integrator	19
II	Computation	21
6	Sequential simulator	23
6.1	Design	23
6.2	Validation	23

6.2.1	Two particle test	24
7	Parallelization techniques	25
7.1	Message Passing Interface	25
7.1.1	Concepts	25
7.1.2	Implementations	26
7.2	OmpSs-2	26
7.2.1	Concepts	26
8	Simulator design	27
8.1	Field solver	27
9	The simulator	29
9.1	Data structures	29
9.2	Simulation flow	29
9.2.1	Initialization	30
9.2.2	Loop	31
9.2.3	Finish	31
10	Analysis	33
10.1	Analysis with varying inputs	34
11	Configuration	35
12	Caveats and limitations	37

Chapter 1

Introduction

It may be surprising to find out that the most common state of matter is plasma when we look at the universe. A plasma is an ionized gas consisting of ions and free electrons distributed over a region in space. in which at least one electron of the atom is separated, so it remains positively charged (ionized) [1]. Usually this happens in the vacuum

1.1 Motivation

1.2 Objectives

1.3 Context

1.4 Structure

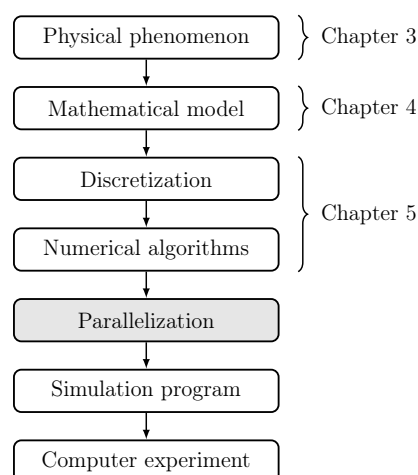


Figure 1.1: Principal steps in computer experiment

The structure of the document follows the diagram shown in the figure 1.1. In chapter 1, plasma is described as a physical phenomenon and we focus on the

relevant properties that we want to study, from which we derive a mathematical model. In chapter 4. The discretization of the mathematical model allows the computer simulation by using numerical algorithms.

Chapter 2

Related work

[Briefly talk about other simulation software and techniques. Also we may want to add some historical references.]

Part I

Theory

Chapter 3

Plasma introduction

Talk about what is a plasma, and why is of interest

Chapter 4

Plasma simulation

4.1 The particle-in-cell method

Solving the Vlasov equation requires a large amount of numerical resources. The particle in cell method, approximates the solution by discretization of the fields.

The method is divided in four main phases:

- Particle motion.
- Charge accumulation.
- Solve field equation.
- Interpolation of fields in particle position.

4.2 Particle mover

In order to move the particles, the equations of motion need to be solved:

$$m \frac{d\mathbf{v}}{dt} = q(\mathbf{E} + \mathbf{v} \times \mathbf{B}) \quad (4.1)$$

$$\frac{d\mathbf{v}}{dt} = \mathbf{v} \quad (4.2)$$

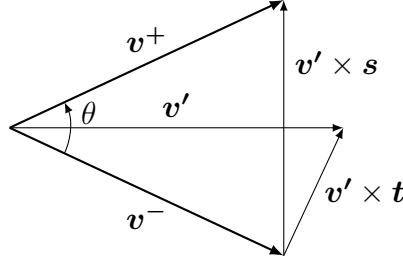
Several methods are available, but we will focus on the Boris integrator.

4.2.1 Boris integrator

Consists of three steps:

1. Add half of the electric impulse
2. Rotate
3. Add the remaining half electric impulse

The Boris integrator computes the velocity of a particle in a constant electric field \mathbf{E} and a constant magnetic field \mathbf{B} . We have the velocity $\mathbf{v}_{t-\Delta t/2}$ of the particle at $t - \Delta t/2$ as we use the leapfrog integrator.

Figure 4.1: Velocity space rotation from $\mathbf{v}-$ to $\mathbf{v}+$

Add half electric impulse We define \mathbf{v}^- as the velocity after half a electric impulse:

$$\mathbf{v}^- = \mathbf{v}_{t-\Delta t/2} + \frac{q\mathbf{E}}{m} \frac{\Delta t}{2}$$

Rotate for the magnetic field The rotation is done in two steps, first the half rotation is computed, with an angle of $\theta/2$:

$$\mathbf{v}' = \mathbf{v}^- + \mathbf{v}^- \times \mathbf{t}$$

Then the rotation is completed by symmetry, using the \mathbf{s} vector

$$\mathbf{s} = \frac{2\mathbf{t}}{1 + \mathbf{t}^2}$$

as

$$\mathbf{v}^+ = \mathbf{v}^- + \mathbf{v}' \times \mathbf{s}$$

4.3 Charge accumulation

The charge density ρ is a scalar field

4.4 Field equations

Once we have the charge density ρ we can compute the electric field \mathbf{E} by the integration of the field equations

$$\mathbf{E} = -\nabla\phi \tag{4.3}$$

$$\nabla \cdot \mathbf{E} = \frac{\rho}{\epsilon_0} \tag{4.4}$$

Which can be combined into the Poisson equation

$$\nabla^2\phi = -\frac{\rho}{\epsilon_0} \tag{4.5}$$

Different methods can be used to obtain the electric field, but we will focus on matrix and spectral methods.

Chapter 5

Discrete model

The mathematical model is discretized in algebraic operations, in order to be computable.

5.1 Charge assignment

At each grid point g at \mathbf{x} we accumulate the charge of each particle p in \mathbf{x}_p as

$$\rho(\mathbf{x}) = \sum_p q W(\mathbf{x} - \mathbf{x}_p) + \rho_0 \quad (5.1)$$

The background charge density ρ_0 is used to neutralize the total charge when is non-zero. The weighting function W determines the shape of the particle charge. Different schemes can be used to approximate the charge density from the particles. We will focus on bilinear interpolation for it's simplicity and low computation requirements. The corresponding weighting function can be written as

$$W(\mathbf{x}) = \begin{cases} \left(1 - \frac{|x|}{\Delta x}\right) \left(1 - \frac{|y|}{\Delta y}\right) & \text{if } -\Delta \mathbf{x} < \mathbf{x} < \Delta \mathbf{x} \\ 0 & \text{otherwise} \end{cases} \quad (5.2)$$

Notice that a particle p always affects the four enclosing grid points in the neighbourhood $\mathcal{N}(p)$, but more complex interpolation methods may extend the update region even further. It may be noted that the increase in smoothing, at computation expense, can gain from the reduced number of particles needed to obtain a similar result, avoiding nonphysical effects. The particle p has a uniform charge area, centered at the particle position \mathbf{x}_p , with size $\Delta \mathbf{x}$, as shown in the figure 5.1. Each grid point A, B, C and D receives the amount of charge weighed by the area a, b, c and d . It can be observed that the area is equal to the opposite region, when the particle p is used to divide the grid cell. The particle shape can be altered later in the Fourier space, without large computation effort, in case the solver already computes the FFT.

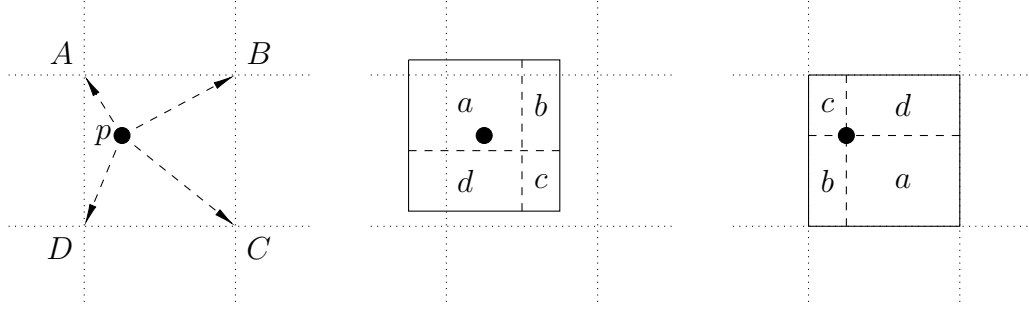


Figure 5.1: Interpolation of particle p charge into the four grid points A to D.

5.2 Field equations

In order to compute the electric field \mathbf{E} , the electric potential ϕ is generally needed, which can be obtained from the charge density ρ .

5.2.1 Electric potential

Several methods are available to solve the Poisson equation (Eq. 4.5).

Iterative methods such as Jacobi, Gauss-Seidel, Successive Over Relaxation (SOR), Chebyshev acceleration are some of the most familiar methods to solve the Poisson equation.

Matrix methods The equations from finite differencing the mesh are considered a large system of equations. We can find in this methods the Thomas Tridiagonal algorithm, Conjugate-Gradient, LU or Incomplete Decomposition.

Spectral methods Also known as Rapid Elliptic Solvers (RES) are a family of methods that use the fast Fourier transform (FFT). Are know for being usually faster than the previous ones, with a complexity in $O(N_g \log_2 N_g)$

We will only focus on the LU for small problems and for testing, and spectral methods, more specific on the Multiple Fourier Transform (MTF) method, as it is the main method implemented in the simulator, due to its relative simplicity and low computational complexity.

5.2.2 LU decomposition

For two dimensions, we can approximate the solution using the second order centered finite differences (with an error proportional to $\Delta x^2 \Delta y^2$), as

$$\frac{\phi(x-1, y) + \phi(x, y-1) - 4\phi(x, y) + \phi(x+1, y) + \phi(x, y+1)}{\Delta x^2 \Delta y^2} = -\frac{\rho(x, y)}{\epsilon_0} \quad (5.3)$$

which leads to a system of N_g linear equations and can be also written in matrix form

$$A\phi = -\frac{\Delta x^2 \Delta y^2 \rho}{\epsilon_0} \quad (5.4)$$

The $N_g \times N_g$ coefficient matrix A has non-zero coefficients only at $a_{ii} = 4$ and $a_{ij} = -1$ with $j \in \{i+1, i-1, i+N_x, i-N_x\} \bmod N_x$, for all $0 \leq i \leq N_g$. However, the matrix A is singular, so the system of equations has infinite solutions. Boundary conditions can be added to get a unique solution. The extra equation $\phi(0,0) = 0$ leads to a system with only one solution, but with one extra equation. In order to keep the matrix A square, the following steps may be taken:

1. Subtract the extra equation $\phi(0,0) = 0$ to the first row of A , with the only change in the coefficient to $a_{11} = 3$.
2. Add all first N_g equations: Each equation has one coefficient of 4 and four of -1 except the first equation. Also we assume the total charge density is zero, obtaining $\phi(0,0) = 0$.
3. Subtract it from the last equation, which leads to a zero coefficient that can be removed.

The only change that remains is at the coefficient $a_{11} = 3$. Now the matrix A is squared and non-singular and has only one solution and can now be solved with the LU method.

The LU decomposition, with a complexity in $O(2/3N_g^3)$, can be used to form two systems of equations that can be solved faster. If we rewrite the system of equations 5.4 as the usual form $Ax = b$ with

$$x = \phi, \quad b = -\frac{\Delta x^2 \Delta y^2 \rho}{\epsilon_0} \quad (5.5)$$

Then we can use the decomposition $A = LU$ to form two systems of equations

$$Ux = y, \quad Ly = b \quad (5.6)$$

which can be solved in complexity $O(2N_g^2)$.

5.2.3 Multiple Fourier Transform (MFT)

The general second-order PDE with constant coefficients and periodic boundary conditions

$$a \frac{\partial^2 \phi}{\partial x^2} + b \frac{\partial \phi}{\partial x} + c\phi + d \frac{\partial^2 \phi}{\partial y^2} + e \frac{\partial \phi}{\partial y} + f\phi = g(x, y) \quad (5.7)$$

can be solved by using the FFT. If we expand ϕ and g in a finite double Fourier series, we obtain

$$\phi(x, y) = \sum_{k,l} \hat{\phi}(k, l) \exp \left(\frac{2\pi i(xk + yl)}{n} \right) \quad (5.8)$$

and

$$g(x, y) = \sum_{k,l} \hat{g}(k, l) \exp \left(\frac{2\pi i(xk + yl)}{n} \right) \quad (5.9)$$

which now can be substituted in the Eq. 5.7, to obtain

$$\hat{\phi}(k, l) = \hat{G}(k, l) \hat{g}(k, l), \quad 0 < k < N_x, 0 < l < N_y \quad (5.10)$$

with for a unit mesh

$$\hat{G}(k, l) = \left[2a \left(\cos \frac{2\pi k}{n} - 1 \right) + ib \sin \frac{2\pi k}{n} + c + \right. \\ \left. 2d \left(\cos \frac{2\pi l}{n} - 1 \right) + ie \sin \frac{2\pi l}{n} + f \right]^{-1} \quad (5.11)$$

To solve the Poisson equation, discretized as Eq. 5.3, we have $a = d = 1$ and $b = c = e = f = 0$ so we can simplify $\hat{G}(k, l)$ as

$$\hat{G}(k, l) = \frac{1}{2} \left[\cos \frac{2\pi k}{n} + \cos \frac{2\pi l}{n} - 2 \right]^{-1} \quad (5.12)$$

Let $g = -\Delta x^2 \Delta y^2 \rho / \epsilon_0$, then the steps to compute the electric potential can be summarized as follows:

$$g \xrightarrow{\text{FFT}} \hat{g} \xrightarrow{\hat{G}} \hat{\phi} \xrightarrow{\text{IFFT}} \phi$$

1. Compute the complex FFT \hat{g} of g
2. Multiply each element of \hat{g} by the corresponding complex coefficient \hat{G} , to obtain $\hat{\phi}$
3. Compute the inverse FFT of $\hat{\phi}$ to get ϕ

The complexity in the worst case is in $O(N_g \log_2 N_g)$ with the number of total points in the grid N_g .

5.2.4 Electric field

The electric field \mathbf{E} can then be obtained by centered first order finite differences in each dimension

$$\mathbf{E}_x(x, y) = \frac{\phi(x-1, y) - \phi(x+1, y)}{2 \Delta x} \\ \mathbf{E}_y(x, y) = \frac{\phi(x, y-1) - \phi(x, y+1)}{2 \Delta y} \quad (5.13)$$

5.3 Force interpolation

The force acting on a particle p can be decomposed in two main parts, the electric and magnetic force $\mathbf{F} = \mathbf{F}_E + \mathbf{F}_B$.

The electric force \mathbf{F}_E is computed similarly as the charge deposition, but in the reverse order. The force \mathbf{F}_E is interpolated from the electric field \mathbf{E} of the neighbour grid points $\mathcal{N}(p)$, using the same interpolation function W .

$$\mathbf{F}_E = q \sum_{g \in \mathcal{N}(p)} W(\mathbf{x}_p - \mathbf{x}_g) \mathbf{E}(\mathbf{x}_g) \quad (5.14)$$

Notice that a particle p only needs the values of the electric field in the neighbourhood $\mathcal{N}(p)$.

The magnetic force \mathbf{F}_B is constant in the simulator, as we only consider a fixed background magnetic field \mathbf{B}_0 . For a particle p with velocity \mathbf{v} can be written as

$$\mathbf{F}_B = q(\mathbf{v} \times \mathbf{B}_0) \quad (5.15)$$

5.4 Equations of motion

In order to move the particles, the equations of motion need to be solved:

$$\frac{d\mathbf{x}}{dt} = \mathbf{v} \quad (5.16)$$

$$m \frac{d\mathbf{v}}{dt} = \mathbf{F} \quad (5.17)$$

The *leap-frog* method is a common integration scheme with second-order accuracy and an error proportional to Δt^2 . The name describes the behavior of the position and velocity, which are updated at interleaved time steps, similarly to the trajectory of a frog. The method is time reversible with a stability far superior of other higher-order integration methods, such as fourth order Runge-Kutta. A more in depth stability analysis can be found in Chapter 4 of Hockney and Eastwood book [3]. The discretized equations can be written as

$$\frac{\mathbf{x}^{n+1} - \mathbf{x}^n}{\Delta x} = \mathbf{v}^{n+1/2} \quad (5.18)$$

$$m \frac{\mathbf{v}^{n+1/2} - \mathbf{v}^{n-1/2}}{\Delta x} = \mathbf{F}(\mathbf{x}^n) \quad (5.19)$$

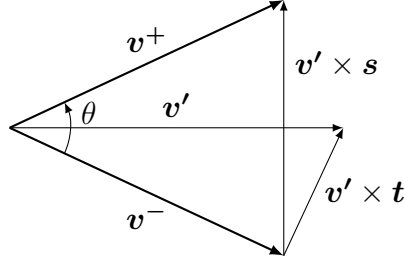
Several methods are available, but we will focus on the Boris integrator.

5.4.1 Boris integrator

Consists of three steps:

1. Add half of the electric impulse
2. Rotate
3. Add the remaining half electric impulse

The Boris integrator computes the velocity of a particle in a constant electric field \mathbf{E} and a constant magnetic field \mathbf{B} . We have the velocity $\mathbf{v}_{t-\Delta t/2}$ of the particle at $t - \Delta t/2$ as we use the leapfrog integrator.

Figure 5.2: Velocity space rotation from $\mathbf{v}-$ to $\mathbf{v}+$

Add half electric impulse We define \mathbf{v}^- as the velocity after half a electric impulse:

$$\mathbf{v}^- = \mathbf{v}_{t-\Delta t/2} + \frac{q\mathbf{E}}{m} \frac{\Delta t}{2}$$

Rotate for the magnetic field The rotation is done in two steps, first the half rotation is computed, with an angle of $\theta/2$:

$$\mathbf{v}' = \mathbf{v}^- + \mathbf{v}^- \times \mathbf{t}$$

Then the rotation is completed by symmetry, using the \mathbf{s} vector

$$\mathbf{s} = \frac{2\mathbf{t}}{1 + \mathbf{t}^2}$$

as

$$\mathbf{v}^+ = \mathbf{v}^- + \mathbf{v}' \times \mathbf{s}$$

Part II

Computation

Chapter 6

Sequential simulator

In order to begin the implementation of the simulator, a initial version was considered with the minimum complexity, to verify the correctness of the model. A graphic subsystem was build with MathGL and OpenGL to produce realtime plots of different elements of the simulation. Of special interests are the particle motion, the electric potential and the electric field.

The language of choice was C for the low overhead, the lack of automatic memory management, the support of different libraries planned in future versions and the low level design, which allowed us to define most of the data structures close to the byte level.

6.1 Design

The simulator initially only supported one group of particles of the same charge and mass, denominated specie. Each particle was implemented as a structure with a given index i , a position vector \mathbf{x} , velocity \mathbf{v} and other extra fields such as the interpolated electric field at the particle position \mathbf{E} . The fields were allocated in contiguous arrays, with the x dimension aligned with the cache line, also called row-major storage.

The configuration of the simulation is specified in plain configuration files, with the syntax defined by the `libconfig` library. Is important to allow the user to specify comments in the configuration files, as well as scientific notation in different values. Additionally, the specification of multiple species benefits from the sub-configuration block feature, which leads to a more intuitive representation. The detailed configuration is described in the chapter 11.

The solver used was initially the LU decomposition, used from the *GSL* numeric library [2], as the only focus was to obtain valid results, ignoring the performance. All implementations are tested beforehand with some test cases designed in `octave`.

6.2 Validation

A set of different tests were designed to determine the correctness of the simulation.

6.2.1 Two particle test

A simple test consists of two electrons placed at some distance different of $L/2$ with no initial speed.

Chapter 7

Parallelization techniques

7.1 Message Passing Interface

From the need of standarize communications in a distributed computing environment, the first draft was proposed in 1992 at the Workshop on Standards for Message Passing in a Distributed Memory Environment, and has now become one of the most used communication protocol in HPC. The Message Passing Interface (MPI) provides a simple to use set of routines to allow processes distributed among different nodes to communicate efficiently.

7.1.1 Concepts

Communicator A communicator refers to a group of processes, in which each has assigned a unique identifier called the *rank*.

Point-to-point communication In order for a process to exchange information with another process, the MPI standard defines what are called point-to-point communication routines. The most common examples are `MPI_Send` to send data, and `MPI_Recv` for the reception. Both routines need the process rank of the process to stablish the connection. Additionally a tag is used to label each message, which can be specified in the reception to filter other messages.

Blocking communication The standard defines various types of communication methods for sending and receiving data. The so called blocking routines are designed such that the call does not return until the communication has been done. In the `MPI_Send` case, the call returns when the sending data can be safely modified, as has been sent or buffered. In the case of `MPI_Recv` the routine only returns when the data has been received.

Non-blocking communication Similarly as with the blocking communication, the routines `MPI_Isend` and `MPI_Irecv` don't wait until the message is sent or received to return. They return immediately, and the communication status can be checked with `MPI_Test` or the process can wait until the communication request has finished with `MPI_Wait`.

7.1.2 Implementations

7.2 OmpSs-2

OmpSs-2 is the next generation of the OmpSs programming model, composed of a set of directives and library routines. Mixes from OpenMP the annotation of source code to parallelize some sections with the StarSs execution model, based on a thread-pool design pattern.

7.2.1 Concepts

Task In OmpSs-2 a task is a section of code that can be executed independently by the runtime schedule. A task may have associated dependencies which lets the scheduler determine in wich order is allowed to execute the tasks. An example annotation of a task:

Parallelization Unless there is a unmet dependency, all tasks ready to run are executed in parallel, up to the number of CPU cores available to the runtime.

Task synchronization It may be possible that at some point in the execution all pending task are required to finish in order to continue. The directive `taskwait` allows the programmer to specify that the runtime must wait for completion of all previous created tasks.

Chapter 8

Simulator design

[After determining the mathematical model and the discretization, we want to begin the discussion on how to build the simulator.]

8.1 Field solver

Talk about MFT and the data layout.

Chapter 9

The simulator

[This chapter is focused on the simulator implementation]

9.1 Data structures

The simulator is designed for space domains of one or two dimensions. In order to parallelize the computation of each step, the space domain is distributed in blocks. First the space domain is split in one specific dimension into MPI blocks, which will be distributed among each compute node. Communications will be needed to share information between MPI blocks.

The second hierarchy splits MPI blocks into task blocks, which can run in parallel inside a compute node. Communications are not needed, as we can use shared memory in the same compute node.

Inside each task block, we have a small portion of the space domain: the grid points of the fields and the particles inside the physical space of the block. Additionally, ghost points are placed at the boundaries of the positive neighbours in each dimension of the problem.

A summary of the data layout can be seen in the figure 9.1, where the physical placement of each block corresponds to the physical position of the grid points. The 1D domain has 2 MPI blocks with 3 task blocks each, and 3 grid points per block with 1 ghost point. In total, the space is discretized in 18 grid points, which require 24 with the ghost points.

Similarly, for 2D the number of ghost points increase, as the frontier now has 2 dimensions, leading to blocks with 6 grid points and 6 ghost points. The whole domain is discretized in 120 grid points, a total of 240 with ghost points.

9.2 Simulation flow

The simulation follows a very precise set of steps to ensure the correct behavior of the physical simulation. Three main stages can be easily identified: Initialization, loop and finish.

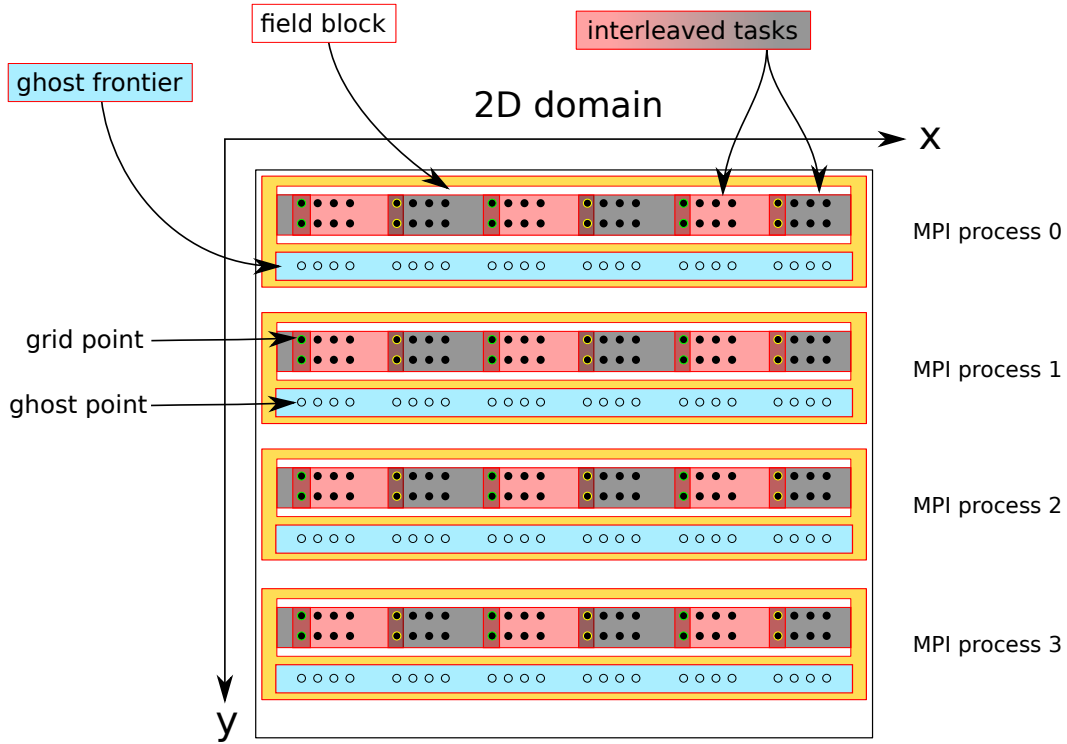


Figure 9.1: Domain blocks

9.2.1 Initialization

The iteration counter is initially set to -2 , as we are going to do two previous phases before the simulation begins:

Allocation phase After P processes were created (as in MPI processes), now we create the different structures to hold the simulation data. First the fields are distributed into task blocks, grouped in each process. For each specie, we distribute the particles based on the particle index p_i , minimizing the difference of the number of particles between blocks. The position, velocity and other parameters are set on each particle, independently of the actual block they reside.

Once all particles are initialized, we begin to move them to the correct block, based on the particle position, and increment the iteration counter. Finally, the charge density field ρ is initially computed, as we want to begin the simulation with the computation of the electric field E from ρ

Rewind phase The simulation time is not advanced equally for the speed and position of the particles. At time t the velocity computed at time $t + \Delta t/2$ whereas the position is computed at time t . In order to begin the simulation, the velocity of the particles is advanced half time-step backwards in time. This extra step is computed at the iteration $i = -1$, as we need the iteration counter to be always increasing (as is used in the message exchange as unique identifier).

9.2.2 Loop

The loop of the simulation perform four main phases:

- Solve field equation to get E from ρ .
- Interpolate E at particle positions E_p .
- Particle motion based on E_p and B_0 .
- Accumulate charge density ρ at the new position of particles.

Solver

We use the MFT method to solve the equation:

$$\nabla^2 E = -\frac{\rho}{\epsilon_0} \tag{9.1}$$

9.2.3 Finish

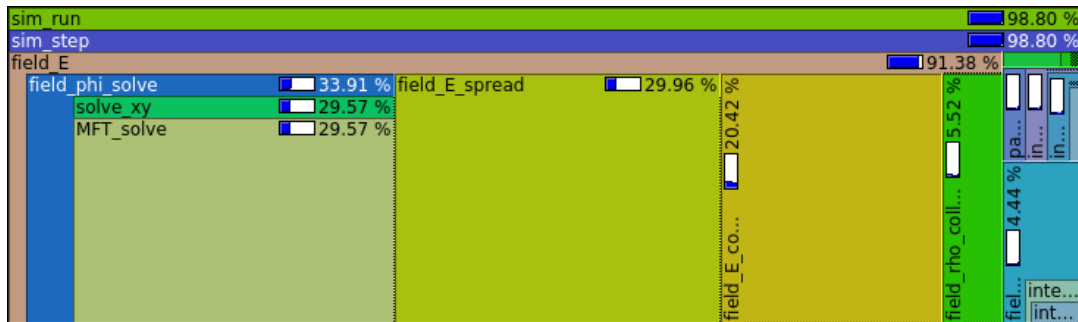
Here we hopefully save some information of the simulation to disk...

Chapter 10

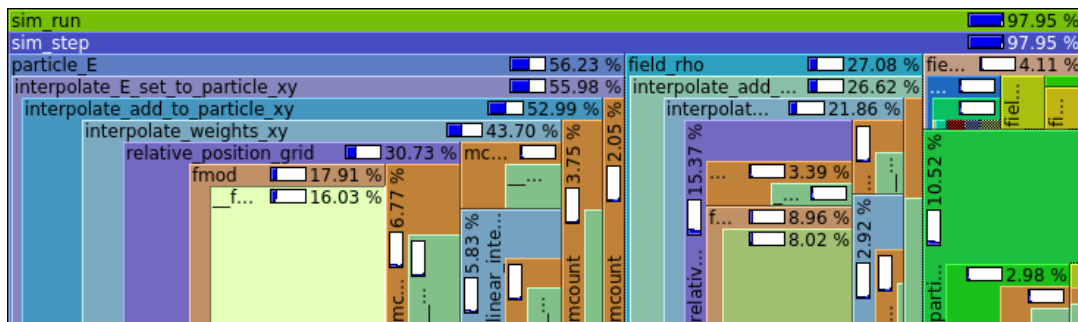
Analysis

In order to reduce the amount of CPU time involved in each step of the simulation, the best strategy is to reduce the time spent in the most time consuming part.

The CPU time involved in each part of the simulation may depend on various factors, such as the number of grid points, the number of particles or the boundary conditions. As an example, consider a simulation with a large number of grid points, with few particles—the computation of the electric field (`field_E`) will dominate the simulation time, as shown in the figure 10.1a. In a case of a large number of particles and a smaller grid, the particle interpolation (`particle_E`) dominates the whole execution as seen in the figure 10.1b. In order to optimize the general use case,



(a) 1024 particles, 512x512 grid points



(b) 10240 particles, 64x64 grid points

Figure 10.1: Comparison of the time spent in each function at two different simulations.

different inputs will be tested and the main simulation steps will be characterized. Furthermore, different algorithms or methods may be used to improve the speed.

As an example, the LU algorithm is compared with the spectral method MFT.

10.1 Analysis with varying inputs

Chapter 11

Configuration

Chapter 12

Caveats and limitations

Here is a list of things that are not implemented in the simulator, but may be added in a future work.

- More than 2 dimensions
- Fully electromagnetic simulation
- Relativistic particle movement
- Heterogeneous architecture (GPU+CPU...)
- Energy conserving codes
- Visualization of big simulations (paraview)
- Replace simulation units, so we avoid factor multiplications
- Other interpolation methods (reduce noise at computational cost)

Caveats that need to be fixed

- Allow to specify plasma frequency
- Validation with other simulation codes

Bibliography

- [1] F. F. CHEN, *Introduction to Plasma Physics and Controlled Fusion: Volume 1: Plasma Physics*, Plenum Press.
- [2] M. GALASSI, J. DAVIES, J. THEILER, B. GOUGH, G. JUNGMAN, P. ALKEN, M. BOOTH, AND F. ROSSI, *GNU Scientific Library Reference Manual*, Network Theory Ltd., third ed., 2009.
- [3] R. W. HOCKNEY AND J. W. EASTWOOD, *Computer Simulation Using Particles*, Taylor & Francis, Inc., Bristol, PA, USA, 1988.